Colloid Polym Sci (2004) 282: 1026–1032
DOI 10.1007/s00396-003-1028-5

ORIGINAL CONTRIBUTION

Susana Shimizu
Paulo Augusto R. Pires
Watson Loh
Omar A. El Seoud

Thermodynamics of micellization of cationic surfactants in aqueous solutions: consequences of the presence of the 2-acylaminoethyl moiety in the surfactant head group

Received: 8 September 2003
Accepted: 12 November 2003

S. Shimizu · P. A. R. Pires
O. A. El Seoud (✉)
Instituto de Química,
Universidade de São Paulo C.P. 26077,
05513-970, São Paulo, SP, Brazil
E-mail: elseoud@iq.usp.br

W. Loh
Instituto de Química,
Universidade Estadual de Campinas,
C.P. 6154, 13083-970 Campinas, SP, Brazil

Abstract The enthalpies of micellization of the following surfactant series have been determined by calorimetry: benzyl (2-acylaminoethyl)dimethylammonium chlorides, *R*ABzMe$_2$Cl, and alkyldimethylbenzylammonium chlorides, *R'*BzMe$_2$Cl, where A, Bz and Me refer to amide, benzyl, and methyl groups, respectively and the acyl (for *R*ABzMe$_2$Cl) and/or the alkyl (for *R'*BzMe$_2$Cl) groups C$_{10}$, C$_{12}$, C$_{14}$, and C$_{16}$, respectively. For both series, the shapes of the calorimetric titration curves (enthalpograms) depend on the following micellar parameters: critical micelle concentration, aggregation number, and degree of counterion binding. The calorimetric-based critical micelle concentrations are in excellent agreement with those determined by conductivity. The Gibbs free energy, the enthalpy and the entropy of micellization were calculated, and divided into contributions from the CH$_2$ groups of the hydrophobic tail, and the terminal CH$_3$ plus head group of the surfactant. For both surfactant series, all thermodynamic parameters per CH$_2$ group were found to be similar, since their transfer (from bulk solution to the micelle) is independent of the surfactant head-group structure. The Gibbs free energy, the enthalpy, and the entropy of transfer of the head group of *R*ABzMe$_2$Cl are more favorable than their counterparts for *R'*BzMe$_2$Cl, because of direct and/or water mediated hygrogen bonding of the amide groups in the micelle.

Introduction

There is intense interest in determining the thermodynamic parameters of micelle formation in aqueous solutions, namely, the Gibbs free energy, ΔG_{mic}, the enthalpy, ΔH_{mic}, and the entropy, ΔS_{mic}, because they quantify the relative importance of hydrophobic interactions, surfactant-water contact and (for ionic surfactants) head-group repulsion. These parameters can be derived from the temperature dependence of the critical micelle concentration (cmc), for example, by application of the van't Hoff equation. Some of the problems that are associated with this approach have been discussed recently [1]; additionally very highly accurate cmcs are required in order to give satisfactory ΔH_{mic}. Among available techniques for studying surfactant aggregation, for example, conductivity, surface tension, and NMR, calorimetry has a distinct advantage, for it is possible to calculate both the cmc and ΔH_{mic} directly from the experimental data. Additionally, the enthalpy and entropy calculated shed light on the balance of forces involved in micelle formation. For example, whereas the aggregation is entropy-driven at room temperature, it is enthalpy-driven at higher temperatures [1]. Introduction of power compensating titration calorimeters, running in the quasi-isothermal mode, has turned titration calorimetry into an attractive technique to study micellization. The reason is that early calorimeters were mostly of the heat-flow type, resulting in very time-consuming experiments.

Recently, we synthesized a novel series of cationic surfactants, namely, benzyl (2-acylaminoethyl)dimethylammonium chlorides, C_nABzMe_2Cl. In this acronym, C_n, stands for an acyl group containing 10–16 carbon atoms, for example, $C_{10}ABzMe_2Cl = C_9H_{19}CONH(CH_2)_2N^+(CH_3)_2CH_2C_6H_5Cl^-$, $C_{12}ABzMe_2Cl$, $C_{14}ABzMe_2Cl$, and $C_{16}ABzMe_2Cl$, where A, Bz and Me stand for the $NH(CH_2)_2N^+$, the benzyl, and the methyl groups, respectively. This series posses several interesting characteristics, namely

1. Owing to the presence of the amide group, they may, in principle, form direct and/or water-mediated intermolecular hydrogen bonds, akin to those formed by *N*-alkylamides and polypeptides [2, 3, 4]. A schematic representation of both types of hydrogen bonding, between the $C=O$ of one surfactant molecule and the N–H group of its neighbor; is shown in Fig. 1.
2. Surfactants that carry the amide group and a (negative) charge, separated by a "spacer", have some interesting interfacial properties, owing to the simultaneous presence of both moieties [5]. We were interested, therefore, in investigating how a similar structural feature (an amide group and a positive charge) affects the solution properties of the series studied.
3. In principle, the micellar interface may be located either at the amide group or at the quaternary ammonium ion of $RCO\text{–}NH(CH_2CH_2)N^+(CH_3)_2Bz\ Cl^-$. Experimentally determined aggregation numbers, and the dependence of the IR frequency of the amide I band on surfactant concentration indicate that the interface lies at the former boundary [6].

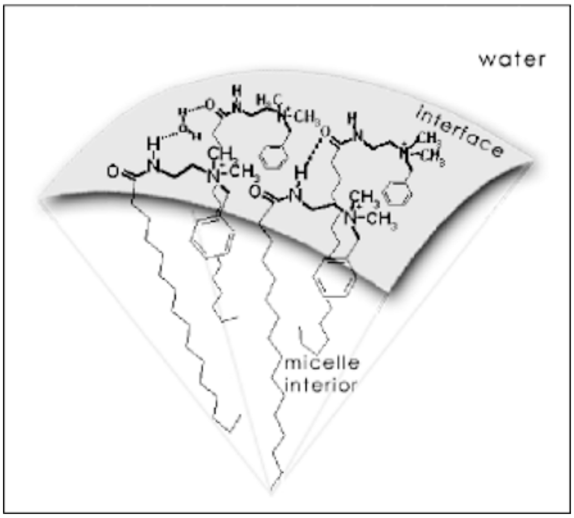

Fig. 1 Schematic representation of direct and water-mediated hydrogen-bonded molecules of $C_{16}ABzMe_2Cl$

We employed surface tension, conductance, electromotive force (chloride ion selective electrode) and Fourier transform IR spectroscopy to study the aggregation of these surfactants in aqueous solutions. The data thus obtained (e.g., cmc, degree of micelle dissociation, and α_{mic}) were compared with those of structurally similar surfactants, except for the absence of the amide group, namely, alkyldimethylbenzylammonium chlorides, $R'BzMe_2Cl$, where Bz and Me are those defined before, and $R' = C_{10}$, $C_{10}BzMe_2Cl$, C_{12}, $C_{12}BzMe_2Cl$, C_{14}, $C_{14}BzMe_2Cl$, and C_{16}, $C_{16}BzMe_2Cl$, respectively. We found that the Gibbs free energies of adsorption and micellization are more favorable for $RABzMe_2Cl$ than for $R'BzMe_2Cl$; this was attributed to the previously mentioned hydrogen bonding (Fig. 1) [6].

We employed calorimetry to study the aggregation of both series in water, at 25 °C. The enthalpy of micellization was obtained directly form experimental data, and ΔG_{mic} and ΔS_{mic} were subsequently calculated. The thermodynamic parameters thus obtained were divided into contributions from the methylene groups of the hydrophobic tail and the head group. As expected, the contribution of the former is insensitive to the structure of the head group. That is, the more favorable ΔG_{mic} of $RABzMe_2Cl$ is essentially due to the transfer of the head group from bulk solution to the micellar pseudo-phase, owing to hydrogen bonding between the surfactant amide groups, in agreement with our previous IR data [6].

Experimental

Materials

The chemicals were purchased from Merck or Fluka. The series $RABzMe_2Cl$ was available from a previous study [6]. Commercial $C_{12}BzMe_2Cl$ was purified by recrystallization from acetone–ethanol, and $C_{10}BzMe_2Cl$, $C_{14}BzMe_2Cl$, and $C_{16}BzMe_2Cl$ were synthesized by reacting the appropriate amount of *N*,*N*-dimethylalkylamine [7] with benzyl chloride in anhydrous acetone. The products were purified by recrystallization from the same solvent, and gave satisfactory elemental analysis (the Elemental Analysis Laboratory, this institute). Double-distilled, deionized water was used throughout.

Titration calorimetry

All experiments were carried out at 25 °C. The enthalpies of micellization of $C_{10}ABzMe_2Cl$ and $C_{12}ABzMe_2Cl$ were measured with a TAM 2277 calorimeter (Thermometric, Järfälla, Sweden). Under constant stirring, 10–20 μl aliquots of the concentrated surfactant solution (surfactant concentration around 20 times the cmc) were added to 2 ml water in the sample cell. Each injection of the titrant solution resulted in a peak, whose corresponding area was calculated with appropriate software. A power-compensated VP-ITC microcalorimeter (Microcal, LLC, Northampton, USA) was used for measurements of $C_{14}ABzMe_2Cl$, $C_{16}ABzMe_2Cl$ and members of the $R'BzMe_2Cl$ series. The procedure was similar to that outlined earlier, except that the measuring cell contained 1.4 ml water.

Solution conductivity

Conductivity measurements were recorded at 25 °C with a personal computer interfaced Fisher model Accumet 50 pHmeter/conductimeter, provided with a Digimed model DM-C1 microconductivity cell (Digimed, São Paulo) and a Schott model Titronic T200 programmed burette. A home-developed software package was used both for programmed dilution of the concentrated surfactant solution and acquisition of conductance data.

Results and discussion

In the following, we discuss the types of calorimetric titration curves obtained, divide the thermodynamic parameters of micellization into contributions from the discrete surfactant moieties, then compare the two surfactant series. Details of the calculations of all the quantities discussed are given in the Calculations section. As shown in the Experimental section, the enthalpy measured is that of demicellization, ΔH_{demic}. It is more common, however, to discuss ΔH_{mic}, whose magnitude is equal to ΔH_{demic}, but with opposite sign.

Typical traces (thermograms) are shown in Fig. 2. Examples of the resultant calorimetric titration curves are shown in Figs. 3 and 4, where the plots are more or less sigmoidal, i.e., can be subdivided into two concentration ranges, with a transition at the cmc region; ΔH_{mic} corresponds to the difference between the extrapolated lines, below and above the cmc.

The calorimetric titration curves of Figs. 3 and 4 have similar shapes; consequently, we examine the former in detail. Figure 3A ($C_{16}ABzMe_2Cl$) shows that the heat of micelle dilution changes sharply in the cmc region; the

Fig. 2 Calorimetric traces (thermograms, heat flow versus time) for **A** $C_{16}ABzMe_2Cl$ and **B** $C_{12}BzMe_2Cl$

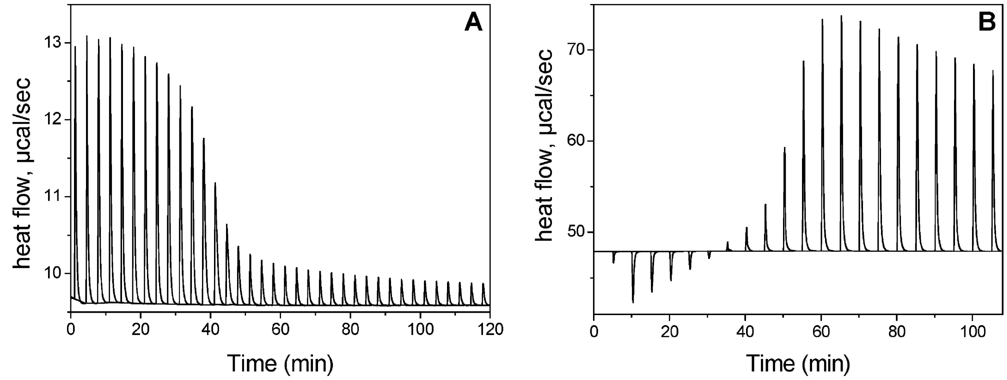

Fig. 3 Calorimetric titration curves for RABzMe$_2$Cl: **A** $C_{16}ABzMe_2Cl$, **B** $C_{14}ABzMe_2Cl$, **C** $C_{10}ABzMe_2Cl$

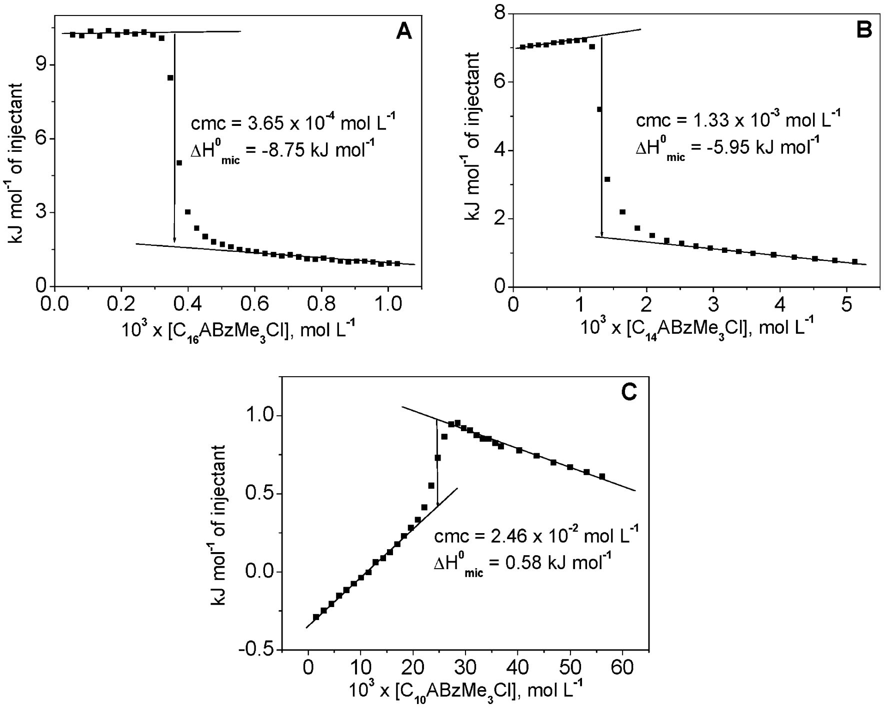

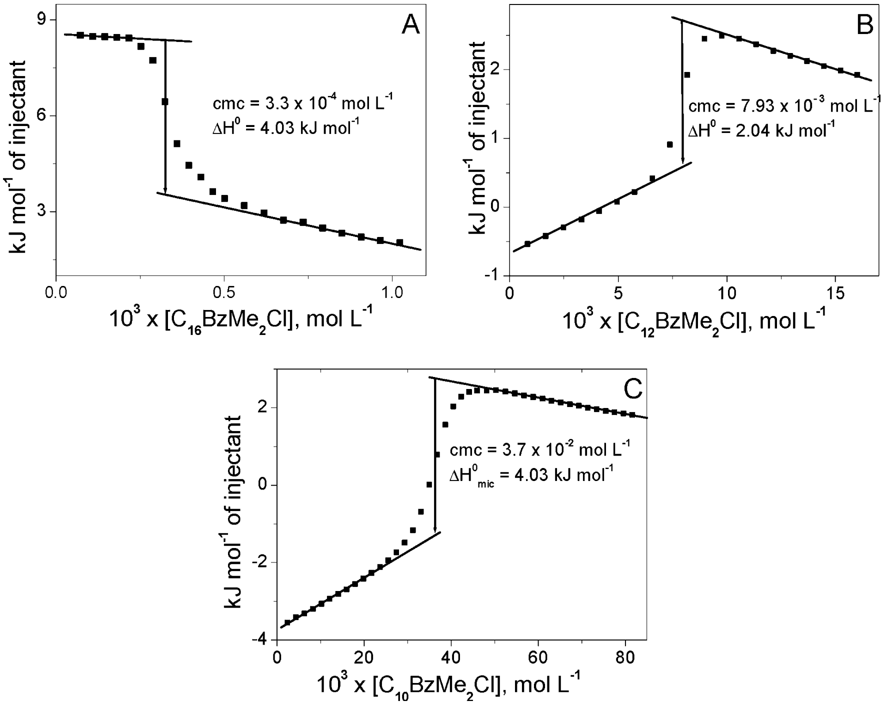

Fig. 4 Calorimetric titration curves for R'BzMe$_2$Cl: **A** C_{16}BzMe$_2$Cl, **B** C_{12}BzMe$_2$Cl, **C** C_{10}BzMe$_2$Cl

two parts of the titration curve (below and above the cmc) are practically independent of solution composition in the sample cell. The change in the cmc region is less sharp in Fig. 3B (C_{14}ABzMe$_2$Cl); the plot shows a small heat dependence on solution concentration. Figure 3C (C_{10}ABzMe$_2$Cl) is complex, since the heat evolution shows a large dependence on the surfactant concentration, below and above the cmc, so visual estimation of this parameter is not feasible. Examples of surfactants that show calorimetric titration curves similar to that of C_{10}ABzMe$_2$Cl (Fig. 3C) include 4-*n*-decylammonium chloride [8], 4-*n*-dodecyl-1-metylpyridinium methylsulfonate, decyltrimethylammonium bromide [9], and disodium 2,2-di-*n*-octyl-1,3-propanediyl bisulfate [10].

The dependence of the shape of the calorimetric titration curve on surfactant structure has been discussed elsewhere, on the basis of the value of the cmc, N_{agg}, and α_{mic} [9]. Small cmc and α_{mic} and large N_{agg} result in an intense heat pulse, either exothermic or endothermic, detected by the calorimeter. A small cmc also means that the solutions in both the sample cell and the injection syringe are essentially ideal (i.e., concentrations are equal to activities), and that the lines before and after the cmc are independent of surfactant concentration, as shown for C_{16}ABzMe$_2$Cl (Fig. 3a). Decreasing the surfactant chain length results in an increase in the cmc and α_{mic}, and a decrease in N_{agg} [6, 11]. Consequently, the surfactant solution in the syringe and, with increasing injection number, in the sample cell cannot be assumed to be ideal. The result is a concentration dependence of the heat evolution, and a smaller enthalpy variation at the cmc, as can be clearly seen by comparing Fig. 3A (C_{16}ABzMe$_2$Cl) and B (C_{14}ABzMe$_2$Cl). For a still shorter hydrophobic chain, the contribution from the nonideal solution properties to the heat of dilution is more significant; the cmc is less well defined and its value may be concentration-dependent (Fig. 3C, C_{10}ABzMe$_2$Cl). A similar line of reasoning applies to R'BzMe$_2$Cl (Fig. 4).

The thermodynamic parameters of micellization were calculated as follows: ΔH_{mic} from calorimetric data, ΔG_{mic} from the cmc and α_{mic}, and ΔS_{mic} from the Gibbs equation. These data are listed in Table 1, from which one concludes the following with regard to aggregation *a*t 25 °C:

1. There is excellent agreement between the cmc (hence ΔG_{mic}) calculated from calorimetry and conductance data, including the C_{10} homologues. This shows that calorimetry is an appropriate technique to probe micelle formation; the derivative method is adequate to calculate calorimetric-based cmcs.
2. Regarding the micellization parameters of a single surfactant, the following is relevant. The contribution of $|\Delta H_{mic}|$ to the Gibbs free energy is much smaller than that of $|T\Delta S_{mic}|$, i.e., micelle formation is entropy-driven, at this temperature. This can be understood in terms of the hydrophobic effect, namely, the large gain in entropy is caused by a decrease in the hydrophobic surface area that is exposed to water, owing to micellization. Additionally, the hydration of the head group upon incorporation

Table 1 Micellization parameters of *R*ABzMe$_2$Cl and *R*′BzMe$_2$ Cl, calculated from calorimetric data, at 25 °C. The values in *parentheses* were calculated from conductivity data [6], at the same temperature

Surfactant	10^3×cmc (mol l^{-1})	ΔG_{mic} (kJ mol^{-1})	ΔH_{mic} (kJ mol^{-1})	$T\Delta S_{\mathrm{mic}}$ (kJ mol^{-1})
C_{10}ABzMe$_2$Cl	24.6 (24.0)	−32.9 (−32.8)	0.58	33.5
C_{12}ABzMe$_2$Cl	6.0 (5.9)	−40.0 (−40.1)	−2.33	37.7
C_{14}ABzMe$_2$Cl	1.33 (1.5)	−46.9 (−46.9)	−5.95	41.0
C_{16}ABzMe$_2$Cl	0.37 (0.40)	−53.4 (−53.0)	−8.75	44.7
C_{10}BzMe$_2$Cl	37.0 (37.3)	−30.4 (−30.4)	4.03	34.5
C_{12}BzMe$_2$Cl	7.93 (8.09)	−38.6 (−38.5)	2.05	40.6
C_{14}BzMe$_2$Cl	2.41 (1.94)	−44.0 (−45.0)	−1.73	42.3
C_{16}BzMe$_2$Cl	0.33 (0.39)	−53.04 (−52.3)	−4.56	48.5

in the micelles is also readjusted according to the surface charge density: a consequence of monomer association and counterion condensation [11, 12].

ΔG_{mic}, ΔH_{mic} and ΔS_{mic} can be divided into contributions from the surfactant discrete groups, as shown by the following example for ΔG_{mic} (Eq. 1). These contributions are from the terminal CH$_3$ group of the hydrophobic chain (ΔG_{CH3}) the methylene groups of the alkyl chain ($N_{\mathrm{CH2}}\Delta G_{\mathrm{CH2}}$), where $N_{\mathrm{CH2}} = 8$, 10, 12, and 14 for *R*ABzMe$_2$Cl and 9, 11, 13, and 15 for *R*′BzMe$_2$Cl, respectively, and the head group ($\Delta G_{\mathrm{head\ group}}$) [11]:

$$\Delta G_{\mathrm{mic}} = N_{\mathrm{CH2}} \times \Delta G_{\mathrm{CH2}} + \Delta G_{\mathrm{head\ group}} + \Delta G_{\mathrm{CH3}}. \qquad (1)$$

Equation (1) predicts a linear correlation between ΔG_{mic} and N_{CH2}, where the intercept includes contributions from its terminal methyl plus the head group. Since ΔG_{CH3} can be considered independent of the chain length of the surfactant, its contribution is constant in a homologous series. Therefore, the intercepts of the plots of two surfactant series essentially reflect effects of the transfer of the appropriate head groups from bulk solution to the micelle, since the contributions of the terminal methyl groups cancel out [11]. A similar line of reasoning, and equations equivalent to Eq. (1), applies to ΔH_{mic} and ΔS_{mic}. Application of Eq. (1) to the data of Table 1 gave the following results (thermodynamic property, correlation coefficient, *r*, for the series *R*ABzMe$_2$Cl, and *R*′BzMe$_2$Cl, respectively): $\Delta G_{\mathrm{mic}} = 0.9998$, 0.9958; $\Delta H_{\mathrm{mic}} = 0.9988$, 0.9937; $T\Delta S_{\mathrm{mic}} = 0.9989$, 0.9799, see Fig. 5. The slopes and intercepts of the plots of Eq. (1) are listed in Table 2.

In analyzing the data of Tables 1 and 2, we consider first the dependence of the thermodynamic parameters on the chain length of the surfactant hydrophobic tail, for the same series. Table 1 shows that this structural variable results in an increase in $T\Delta S_{\mathrm{mic}}$ and a decrease in ΔH_{mic}. Increasing the chain length of the surfactant results in

1. An increase in the contribution of hydrophobic hydration; this explains the entropy change.
2. An increase in N_{agg}, with a concomitant closer packing of surfactant molecules in the aggregate. This results in a favorable enthalpy change, owing to stronger London dispersion interactions between the hydrophobic moieties, and less water penetration between the head groups. Note that the accompanied increase in head-group repulsion is attenuated by an increase in counterion binding [13].

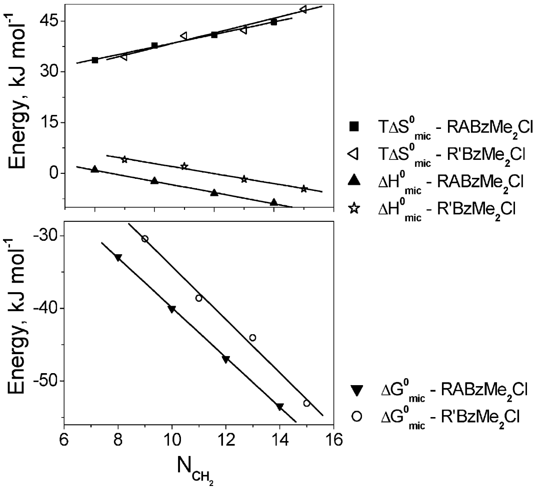

Fig. 5 Thermodynamic parameters of micellization versus the number of CH$_2$ groups of the acyl and alkyl chains, N_{CH2}, of *R*ABzMe$_2$Cl and *R*′BzMe$_2$Cl, respectively

We now address the differences between the thermodynamic parameters of the two series. The consequence of the presence of the amide group in *R*ABzMe$_2$Cl is best discussed by considering the contribution of the discrete surfactant segments to the parameters of transfer of the surfactant monomer, from bulk aqueous phase to the micelle, see Table 2. We focus on the CH$_2$ group and the head group, since the contribution of CH$_3$ cancels out, as already discussed. As Table 2 shows, all parameters of transfer of the CH$_2$ groups are similar for the two surfactant series, since this process is practically independent of the structure of the head group [11]. The following additional data show that the energetics of transfer of the CH$_2$ group, for a variety of systems, are structure-independent, i.e., their values are similar to those listed in Table 2: ΔG_{CH2} for the transfer of alkanes from water to bulk hydrocarbon

Table 2 Contribution of the surfactant discrete segments to the thermodynamic parameters of micellization (kJ mol), at 25 °C

Surfactant	ΔG_{CH2}	ΔH_{CH2}	$T\Delta S_{\mathrm{CH2}}$	$\Delta G_{\mathrm{CH3+head\ group}}$	$\Delta H_{\mathrm{CH3+head\ group}}$	$T\Delta S_{\mathrm{CH3+head\ group}}$
*R*ABzMe$_2$Cl	−3.42	−1.58	1.84	−5.64	13.3	18.9
*R′*BzMe$_2$Cl	−3.66	−1.48	2.19	2.44	17.7	15.2

is −3.56 kJ mol^{-1} [14]; ΔH_{CH2} (micellization) is −1.4, –1.1, and −1.5 kJ mol^{-1}, for *n*-alkylmethylsufoxides, *n*-alkyldimethylphosphine oxides, and *N*-alkylpyridinium bromides, respectively [15, 16]; for the first two surfactant series, the corresponding $T\Delta S_{\mathrm{CH2}}$ are 1.87 and 2.04 kJ mol^{-1}, respectively [15]. In contrast, the Gibbs free energy of transfer of the head group of *R*ABzMe$_2$Cl is much more favorable than the corresponding one of *R′*BzMe$_2$Cl, a consequence of the smaller (i.e., less unfavorable) $\Delta H_{\mathrm{CH3+head\ group}}$ and larger (i.e., more favorable) $T\Delta S_{\mathrm{CH3+head\ group}}$. In order to explain this result, the contribution (to the parameters of transfer) of two factors is considered, namely, hydrogen bonding and conformations of surfactant molecules. IR frequencies of the amide I band of *R*ABzMe$_2$Cl have indicated that this group is hydrated in the monomeric state; some of this water of hydration is lost in the micelle, presumably because of hydrogen bonding [6]. Owing to this desolvation, the transfer of the surfactant head group from bulk water to the interfacial region is expected to be endothermic, in agreement with the fact that the enthalpy of transfer of quaternary ammonium ions from water to aqueous organic solvents is positive [17]. A part of this endothermicity is compensated by (exothermic) hydrogen bonding, in agreement with the fact that $\Delta H_{\mathrm{CH3+head\ group}}$ (*R*ABzMe$_2$Cl) < $\Delta H_{\mathrm{CH3+head\ group}}$ (*R′*BzMe$_2$Cl). Hydrogen bonding releases water of hydration, thus contributing to the larger $T\Delta S_{\mathrm{CH3+head\ group}}$ of *R*ABzMe$_2$Cl. NMR data have indicated the following picture for both surfactant series. Below the cmc, the monomers have a compact (i.e., coiled) rather than an extended shape; on aggregation, the benzyl group folds back toward the micelle interior [6, 18, 19]. That is, monomer transfer from bulk solution to the micelle is accompanied by an increase in the degrees of freedom, resulting in positive $T\Delta S_{\mathrm{mic}}$. Flexibility of the "tether" to which the benzyl group of *R*ABzMe$_2$Cl is attached probably plays an additional part in the entropy change, since the degree of freedom of the $-(CH_2)_2N^+(CH_3)_2CH_2C_6H_5$ moiety is most certainly larger than the relatively constrained $-N^+(CH_3)_2CH_2C_6H_5$ group.

Conclusions

Calorimetry is a useful technique for the determination of the thermodynamics of micellization of surfactants, and in probing the effects of their structures on the properties of the aggregates formed. The surfactant series studied differ in the structure of their head groups. Formation of hydrogen bonds and differences in monomer conformations in the micelle attenuate the enthalpy and increase the entropy of transfer of *R*ABzMe$_2$Cl molecules from bulk solution to the aggregate, resulting in more favorable Gibbs free energies of micellization.

Calculations

Critical micelle concentration

The cmc is usually taken as the concentration where the first derivative of the calorimetric titration curve displays a minimum, or a maximum, depending on the surfactant. One problem is the small number of experimental points in the cmc region, a consequence of the abrupt rise of the enthalpy as a function of the surfactant concentration, for example, Fig. 3a and b. To avoid this problem, and to improve the precision of the cmc calculated, we fitted the heats of dilution versus surfactant concentration curves with Eq. (2) [20]:

$$H_{\mathrm{dil}} = \frac{a_1 c + a_2}{1 + \exp\left[\frac{(c - a_3)}{\mathrm{d}x}\right]} + a_4 c + a_5, \tag{2}$$

where c is the surfactant concentration and a_1–a_5 are fitting parameters. Although the initial guesses of the latter parameters have not been specified in the literature [20], they should be, in part, related to the physicochemical change that is being measured. We found that the best fit was obtained by taking, as initial guesses, $a_1 = a_4 = a_5 = 1$, $a_2 = \Delta H_{\mathrm{mic}}$, $a_3 = \mathrm{cmc}$ and $\mathrm{d}x = \Delta_{\mathrm{cmc}}$. The latter variable refers to the width of the transition studied [21], and was taken as ±15% of the cmc. In all cases, iteration-based a_2 and a_3 were in agreement with their initial guesses. The cmc values reported were taken as the maximum, or minimum, of the first derivative of Eq. (2).

Aggregation number

N_{agg} was calculated from the length of the surfactant monomer and the diameter of the (spherical) aggregate by assuming that the monomer has a stretched, all-trans conformation within the micelle (Spartan-Pro program package, version 5.1, Wave Function, Irvine, CA). As already discussed, the micellar interface of *R*ABzMe$_2$Cl was considered to lie at the amide nitrogen atom, whereas for $R'\mathrm{BzMe_2Cl}$ [$R'\mathrm{N^+(CH_3)_2CH_2C_6H_5\ Cl^-}$] it lies at the quaternary nitrogen. N_{agg} values for both series were found to be 43, 61, 82, and 107 for RCO and/or $R' = 10$, 12, 14, and 16, respectively [6].

Degree of micelle dissociation

This was calculated by the Evans method (Eq. 3) [22]:

$$1000S_2 = \frac{\alpha_{\mathrm{mic}}^2}{N_{\mathrm{agg}}^{-2/3}}(1000S_1 - \Lambda_{\mathrm{Cl^-}}) + \alpha_{\mathrm{mic}}\Lambda_{\mathrm{Cl^-}}, \tag{3}$$

where S_1, S_2, and $\Lambda_{\mathrm{Cl^-}}$ refer to the slopes of the conductance plot below and above the cmc and the equivalent conductance of the surfactant counterion at infinite dilution, respectively. For the series $R\mathrm{ABzMe_2Cl}$, the α_{mic} values were those reported elsewhere [6]. The corresponding values for R'BzMe2Cl, measured in the present work, were found to be 0.32, 0.24, 0.23, and 0.22 for $\mathrm{C_{10}BzMe_2Cl}$, $\mathrm{C_{12}BzMe_2Cl}$, $\mathrm{C_{14}BzMe_2Cl}$, and $\mathrm{C_{16}BzMe_2Cl}$, respectively.

Thermodynamic parameters of micellization

The Gibbs free energy and the entropy of micelle formation were calculated from Eqs. (4) and (5):

$$\Delta G_{\mathrm{mic}} = (2 - \alpha_{\mathrm{mic}})RT\ln\chi_{\mathrm{cmc}}, \tag{4}$$

$$T\Delta S_{\mathrm{mic}} = \Delta H_{\mathrm{mic}} - \Delta G_{\mathrm{mic}}, \tag{5}$$

where χ_{cmc} is the cmc on the mole fraction scale, and ΔH_{mic} is that calculated from calorimetry.

Acknowledgements We thank the São Paulo State Research Foundation, FAPESP, for financial support and for a predoctoral fellowship to S.S., and the National Research Council, CNPq, for a research productivity fellowship to O.A.E.., and Rodrigo C. Silva for help with calorimetric measurements in the initial stage of this work.

References

1. Chatterjee A, Moulik SP, Sanyal SK, Mishra BK, Puri PM (2001) J Phys Chem B 105:12823
2. Kollman P (1993) Chem Rev 93:2395
3. Ludwig RO, Winter R, Weinhold F, Farrar TC (1998) J Phys Chem B 102:9312
4. Huelsekopf M, Ludwig R (2001) Magn Res Chem 39:127
5. Tsubone K, Rosen MJ (2001) J Colloid Interface Sci 244:394
6. Shimizu S, El Seoud OA (2003) Langmuir 19:238
7. Reck RA, Harwood HJ, Ralston AW (1947) J Org Chem 12:517
8. Mehrian T, de Keizer A, Korteweg AJ, Lyklema J (1993) Colloids Surf A 71:255
9. Bijma K, Engberts JBFN, Blandamer MJ, Cullis PM, Last PM, Irlam KD, Soldi LG (1997) J Chem Soc Faraday Trans 93:1579
10. Kooreman S (1995) PhD thesis. University of Groningen
11. (a) Rosen MJ (1989) Surfactants and interfacial phenomena. Wiley, New York, p 33; (b) Hiemenz, PC, Rajagopalan (1997) Principles of colloid and surface chemistry, 3rd edn. Dekker, New York, pp 297, 355
12. (a) Tanford C (1980) The hydrophobic effect: formation of micelles and biological membranes, 2nd edn. Wiley, New York; (b) Blokzijl W, Engberts JBFN (1993) Angew Chem 32:1545
13. Bijma K, Blandamer MJ, Engberts JBFN (1998) Langmuir 14:79
14. Nelson HD, de Ligny CL (1968) Rec Trav Chim 87:528
15. Clint JH, Walker T (1974) J Chem Soc Faraday Trans I 71:946
16. Lah J, Pohar C, Vesnaver G (2000) J Phys Chem B 104:2522
17. Hefter G, Marcus Y, Waghorne (2002) Chem Rev 102:2773
18. Rózycka-Roszak B, Cierpicki T (1999) J Colloid Interface Sci 218: 529
19. Shimizu S, Pires PAR, Fish H, Halstead TK, El Seoud OA (2003) Phys Chem Chem Phys 5:3489
20. Király Z, Dekány I (2001) J Colloid Interface Sci 242:214
21. Carpena P, Aguiar J, Bernaola-Galván P, Ruiz CC (2002) Langmuir 18:6054
22. Evans HC (1956) J Chem Soc 579